Some Mesoscale Aspects of the 6 June 1990 Limon, Colorado, Tornado Case

JOHN F. WEAVER AND JAMES F. W. PURDOM†

Regional and Mesoscale Meteorology Branch, NOAA/NESDIS, Fort Collins, Colorado

EDWARD J. SZOKE*

NOAA Forecast Systems Laboratory, Boulder, Colorado

(Manuscript received 19 January 1993, in final form 3 September 1993)

ABSTRACT

During the late afternoon and early evening of 6 June 1990, a series of severe thunderstorms produced nine tornadoes and numerous incidents of large hail on the High Plains of eastern Colorado. While the morning synoptic data clearly indicated a severe threat over the entire eastern half of the state, the severe activity that did occur was much more localized. Significant events were confined to a relatively small geographical region east and southeast of Denver, Colorado, including the small town of Limon some 70 miles to its southeast.

Satellite, radar, surface, and upper-air data are combined in this paper to study some of the mesoscale aspects of the severe storm environment. Results show that thunderstorm outflow from a large mesoscale convective system in Kansas and Nebraska played a crucial role in focusing the severe activity in eastern Colorado. Also, the evolution of convective development during the early part of the day suggested the presence of a sharp moisture gradient along the Front Range of the Rocky Mountains, which further helped to localize the outbreak. Finally, interactions between individual storms appear to have been critical to severe storm evolution.

1. Introduction

During the late afternoon and early evening of 6 June 1990 a series of severe thunderstorms produced numerous incidents of hail up to 6.3 cm (2.5 in.) in diameter, torrential rain, and at least nine tornadoes (NOAA 1990) across the plains of eastern Colorado. Although the region is sparsely populated, the event was significant in this case, since a 0.4-km-(0.25 mile) wide F3-intensity tornado (Fujita 1971) struck the small town of Limon, causing $12.8 million in damage and injuring 14 people. Most of the buildings along the main street of the town were destroyed.

The outbreak was well forecast on the synoptic scale. The purpose of this paper is to present a review of the case using visible and infrared satellite imagery, radar data, and other supplementary information to identify mechanisms that helped focus the severe weather. The data clearly show that an early morning mesoscale convective system played an important role in later storm evolution and that interaction between individual thunderstorms was particularly crucial to the events that unfolded.

2. Morning conditions—0330 to 1100 local standard time (LST)

Synoptic conditions on the morning of 6 June 1990 (Fig. 1) fit all the criteria to qualify it as a "classic" High Plains, severe weather day (Doswell 1980). The 500-mb flow over the region was from the west-southwest at 15–17 m s^{-1} (30–35 kt), and a moderately strong short-wave trough was approaching from the west. Notice, for example, the cold-air advection over Colorado at 500 mb, or that the state appears to be in the right entrance region of a jet streak at 300 mb. Furthermore, morning surface analysis showed that a synoptic-scale cold front had pushed through most of the state early on the previous day, leaving northeastern Colorado in low-level southeasterly flow. This is an upslope situation and on 6 June was causing strong, low-level moisture advection to occur. By 0500 LST, dewpoints of 10°C (50°F) could be found as far west as the cities just east of the Rocky Mountain Front Range. (See Fig. 2 for all geographical references.)

Figure 3 presents both an analysis of the 0500 LST pressure field (reduced to 1500 m) as well as a more detailed analysis of surface dewpoints at that time. The analysis was carried out using the Mesoscale Analysis and Prediction System (MAPS) routine, which was designed by the National Oceanic and Atmospheric

† Other affiliation: The Cooperative Institute for Research in the Atmosphere, Colorado State University, Fort Collins, Colorado.

* Other affiliation: The National Center for Atmospheric Research, which is sponsored by the National Science Foundation.

Corresponding author address: John Weaver, NOAA/NESDIS/RAMM Branch CIRA, W. Laporte Avenue, Colorado State University, Fort Collins, CO 80523.

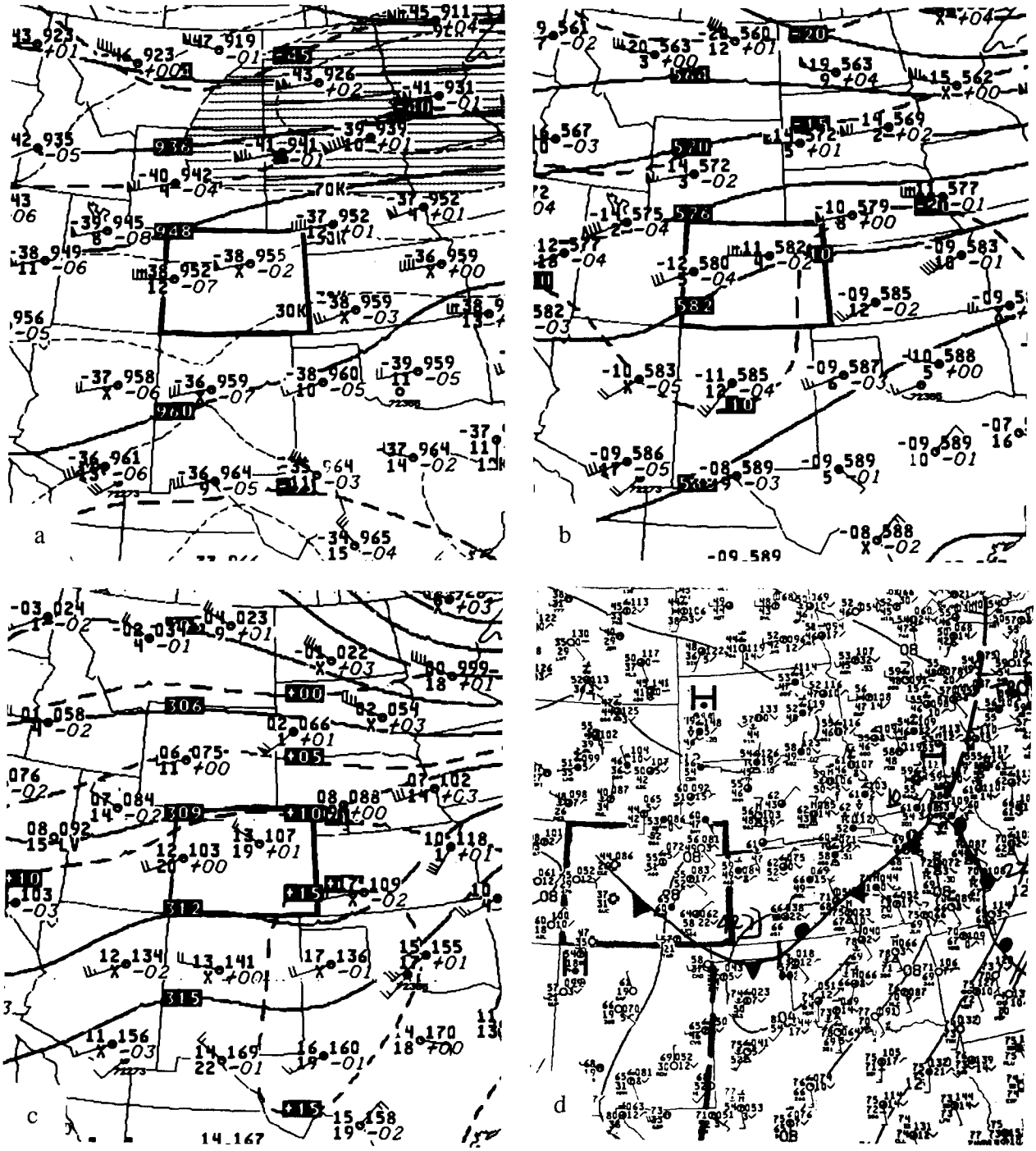

FIG. 1. Photocopies of synoptic analyses from 0500 LST 6 June 1990. Levels shown are (a) 300 mb, (b), 500 mb, (c) 700 mb, and (d) surface. In (a), (b), and (c), solid lines are heights in decameters and dashed lines are temperatures in degrees celsius. Surface plots are in conventional (English) units. Wind barbs are as follows: flags = 25 m s^{-1} (50 kt), full barbs = 5 m s^{-1} (10 kt), and half barb = 2.5 m s^{-1} (5 kt).

Administration's (NOAA's) Forecast System Laboratory. For a description of the system refer to Benjamin and Miller (1990) or Miller and Benjamin (1992). Noteworthy from the dewpoint analysis is the generally moist air over eastern Colorado, with a tongue of high surface moisture extending northwestward from southeast Kansas to the Palmer Lake Divide. By contrast, notice the extremely dry air over the higher terrain

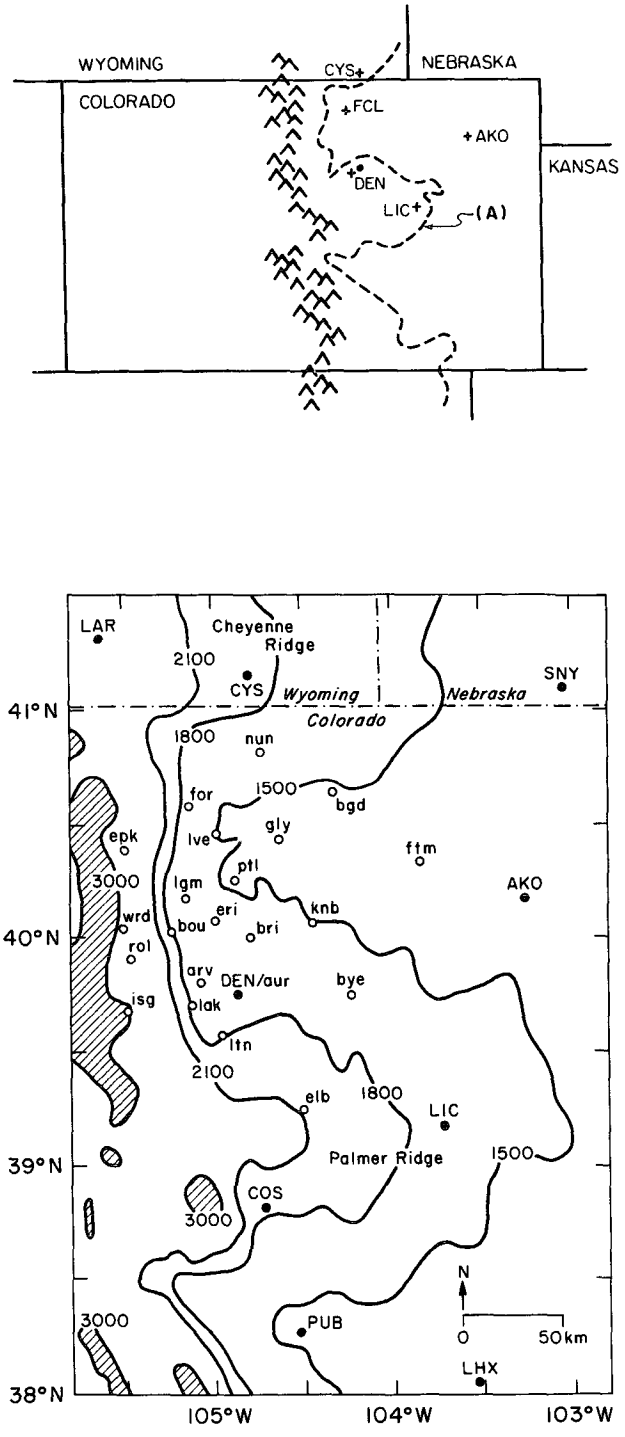

FIG. 2. (a) Topography of Colorado and surrounding vicinity. Schematic shows 1500-m terrain contour (dashed) and several cities referred to in text. The small dot northeast of DEN marks the location of the Mile-High Doppler radar. The approximate location of the so-called Front Range of the Rocky Mountains is indicated by the line of carats. Feature "A" is the Palmer Lake Divide. Panel (b) is the detail of northeast Colorado showing 1500-m, 1800-m, 2100-m, and 3000-m terrain contours as well as the locations of NWS and Program for Regional Forecasting and Observing Systems mesonet sites referred to in text.

to the west. This implied vertical structure agrees with the shallow moist layer shown by the Denver morning sounding taken at this time (Fig. 4a). That is, the surface data supports the idea of a shallow, surface-based moist layer developing due to the low-level upslope flow.

It should also be noted that the horizontal gradient in the surface dewpoint data might seem even more marked than that shown by the MAPS analysis, since the objective scheme does not appear to properly account for the 10°C (50°F) dewpoints at Denver, Colorado (DEN), Fort Collins, Colorado (FCI) or Cheyenne, Wyoming (CYS). Thus, the MAPS analysis at 0500 LST seems to underplay the amount of moisture along the Front Range. However, as we shall see in a short while, that is not entirely true.

To summarize, the presence of low-level upslope flow, dewpoints greater than 7°C (45°F), and westerly 500-mb winds greater than 10 m s^{-1} (20 kt) represent the conditions associated with the majority of severe thunderstorm events in eastern Colorado (Doswell 1980; Weaver and Doesken 1991). The synoptic environment on 6 June 1990 included all of these, along with a moderately strong short-wave trough entering Colorado from the west.

The morning Denver radiosonde data (Fig. 4a) did not show evidence of much low-level, vertical wind shear. Storm-relative helicity (Davies-Jones et al. 1990) calculated from the Denver radiosonde winds, with an estimate of storm motion based on the method of Leftwich (1990), results in an extremely low value of 18 $(m\ s^{-1})^2$. This is far below the empirically derived mean value for weak mesocyclones of 278 $(m\ s^{-1})^2$ that Davies-Jones et al. (1990) found in a study involving 28 tornadoes of varying strengths.

By contrast, the late afternoon shear profile, especially that just east of Denver, was expected to be considerably more favorable, since southeasterly surface winds of 5–8 m s^{-1} (10–15 kt) were expected to develop. Indeed, post-storm analysis found that when late afternoon Denver radiosonde observations (Fig. 4b) are combined [by linear extrapolation through a depth of 100 mb above ground level (AGL)] with observed afternoon surface winds near Limon, Colorado (LIC), and when storm motion vectors representative of what actually occurred are used in helicity calculations, the estimated storm-relative helicity near LIC ranges from 250 to 350 $(m\ s^{-1})^2$. This range of values is favorable for mesocyclone production (although lower-end values are marginal).

Conditional instability was expected to be extremely high. When a lifted parcel, based on a forecast afternoon temperature and mixed dewpoint of 29.5°C (85°F) and 11°C (52°F), respectively, is used in combination with the Denver morning radiosonde data (Fig. 4a), the value of the resulting positive Convective Available Potential Energy (CAPE) is approximately 3000 J Kg^{-1}. These values were representative of con-

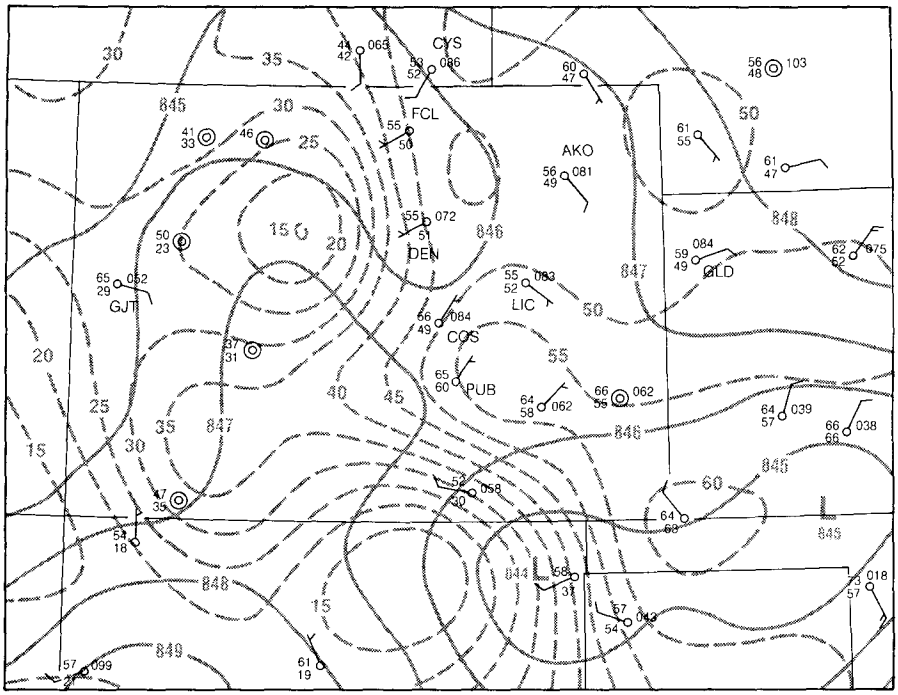

FIG. 3. The MAPS analysis of the pressure field reduced to 1500 m (solid lines) and surface dewpoints (dashed) for 0500 LST on 6 June 1990. Temperatures and dewpoints are in degrees Fahrenheit; pressure is in millibars. Wind barbs are as in Fig. 1.

ditions near storm time and location. Note that when such a parcel is combined with the estimated late afternoon shear profile, the bulk Richardson number (Weisman and Klemp 1982) comes out to about 40. This value is considered to be the threshold-separating supercell from multicell storms.

Figure 5 shows a portion of the 0800 LST National Meteorological Center (NMC) surface analysis focusing on Colorado and its vicinity. Notice the moist, upslope flow over the eastern half of the region and the rather weak pressure gradient driving it. Also notice what appear to be relatively homogeneous surface airmass characteristics over northeastern Colorado. Actually, the low-level air mass was far from homogeneous. A great deal of the rest of this paper will focus on the evolution of the mesoscale components of the lower troposphere over northeastern Colorado. In fact, one extremely important component was just entering the state at the time of this map.

During the predawn hours of the outbreak day, much of northern Kansas and western Nebraska had been covered with convection (e.g., Fig. 6). This activity resulted in a widespread area of relatively stable air that began pushing westward after sunrise. Low-level stratocumulus billows could be seen in visible satellite imagery during the morning hours within a large portion of this thunderstorm-modified air mass (Fig. 7), particularly the region near its western edge. These "billow clouds" are the same phenomenon described as "stable wave clouds" in Scofield and Purdom (1986) and Purdom (1990).

With clues offered by radar summaries, satellite imagery, and the supposition that this shallow front would most likely have not been able to spill over the high terrain of the Front Range, a reanalysis of Fig. 5 is possible (Fig. 8). To extract even more detail, the reanalysis was done using a 1-mb pressure increment. A cautionary note—the mesoscale pressure features shown to the west of the front are most probably artifacts of pressure reduction errors induced by the complex terrain over the Rocky Mountains, while that portion of the analysis to the east (right) of the front provides a relatively accurate analysis of the routinely analyzed surface variables. However, it is important to point out that the reanalysis offers only a slight improvement in picking out specifically threatened areas. We present this map simply as a more detailed version of the standard.

Because the western edge of the mesoscale outflow air mass continued to be marked by stable stratocumulus billows, satellite imagery could be used to track its westward progress as it moved into northeastern Colorado throughout the morning. The encroaching air was marked by a negative temperature anomaly on infrared satellite imagery (on the order of $-10°C$ in the rain-modified air) and by a slight increase in surface dewpoints. As the edge of this feature reached Akron, Colorado (AKO), the dewpoint rose 2.5°C (5°F), and

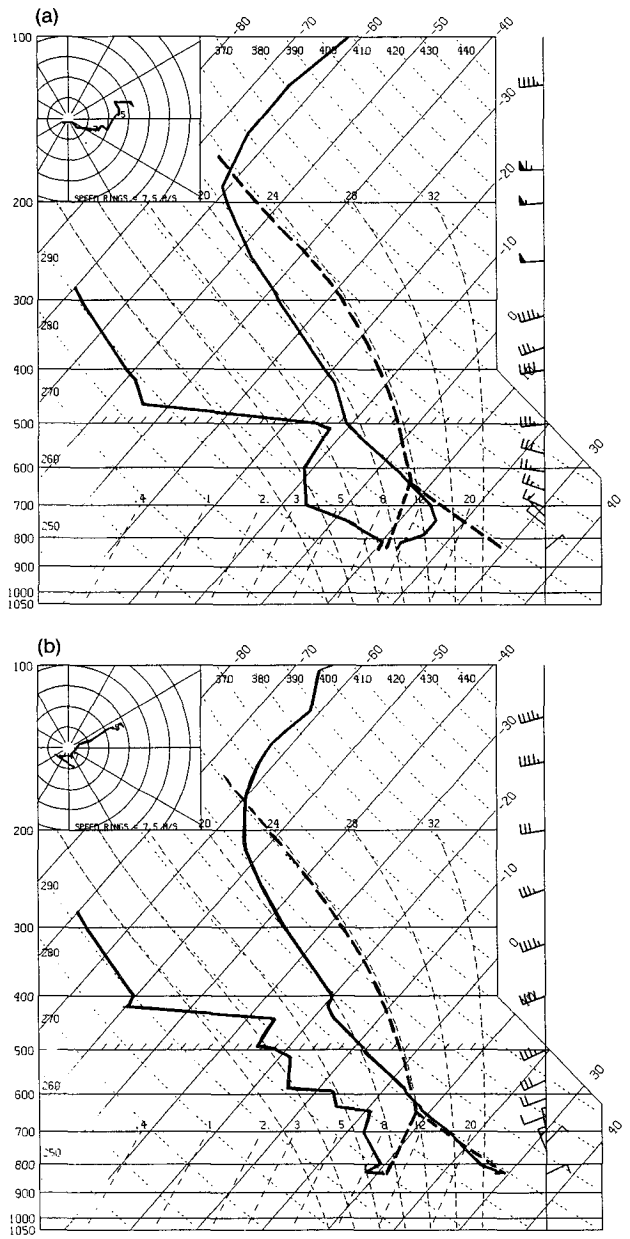

FIG. 4. The 6 June 1990 rawinsonde data from Denver plotted on skew T–log$p$ diagrams. Panel (a) is from the 0500 LST release, and panel (b) is from 1700 LST. Solid lines are temperature (right) and dewpoint (left). The dashed line represents an estimated afternoon surface lifted parcel lapse rate. Wind barbs are as in Fig. 1.

reported cloud cover went from "10 000 ft., scattered" to "8000 ft., broken." The surface temperature at Akron did not decrease at the time of the boundary passage. However, for the rest of the day, heating was suppressed behind the boundary, even though the cloud cover decreased. Afternoon surface temperatures at Akron ended up being several degrees cooler than those reported by nearby stations not affected by the mesoscale outflow.

3. Midday development

a. 1100—1300 LST

A terrain-induced convergence boundary, called the Denver Convergence and Vorticity Zone (DCVZ) (Szoke et al. 1984), often plays an important role in the formation and/or intensification of deep convection in Colorado (e.g., Szoke and Augustine 1990). A mesonetwork of 22 surface observing sites (Fig. 2b), installed in 1980 by the Program for Regional Observing and Forecasting Services (PROFS), provides 5-min interval surface observations over northeastern Colorado. This network has allowed for detailed study of the DCVZ phenomenon. Also, data from this network are routinely available to weather forecasters at the Denver Weather Service Forecast Office (WSFO). The dashed line in Fig. 7 shows the approximate, climatologically favored location for DCVZ formation.

By late morning, surface data strongly suggested that a well-defined DCVZ was forming (Fig. 9). Because the convergence and cyclonic vorticity between the southerly flow east of the DCVZ and the northerly flow to its west were similar to past convective events in which the phenomenon played a key role, the attention of many local forecasters was focused on that region for first storm development east of the Rockies. Additionally, the presence of the DCVZ was the primary reason for the National Severe Storms Forecast Center's including the Denver metropolitan area in a tornado watch for later that afternoon. (The third author was working as shift forecaster at the Denver WSFO on this day.)

However, the first deep convection did not develop along the DCVZ. Between 1200 and 1230 LST, visible satellite imagery detected a cluster of towering cumulus about 50 km (30 miles) northwest of LIC. By 1300 LST these towers had grown into two small thunderstorms (Fig. 10). The activity had apparently formed along a ridge of low-level, warm, moist air situated over eastern Colorado (Fig. 11), where it intersected the northern side of a terrain feature called the Palmer Lake Divide ("A" in Fig. 2).

Convective cloud climatologies (e.g., Klitch et al. 1985) find that the higher terrain comprising the Palmer Lake Divide is a favored area for thunderstorm formation, so it is not surprising that convective development occurred at that location. What is unusual is that deep convection did not develop first where the Palmer Divide intersects the higher terrain to the west (as normally occurs), particularly since a DCVZ had formed.

Several clues are available to help explain the apparent anomaly. The supporting data all suggest that the lowest 1000 m, or so, of the atmosphere close to the Front Range were drier than that a little farther east. First, the morning radiosonde data showed shallow moisture at DEN (Fig. 4a). Second, Figs. 9 and 11 both show a sharp gradient of surface mois-

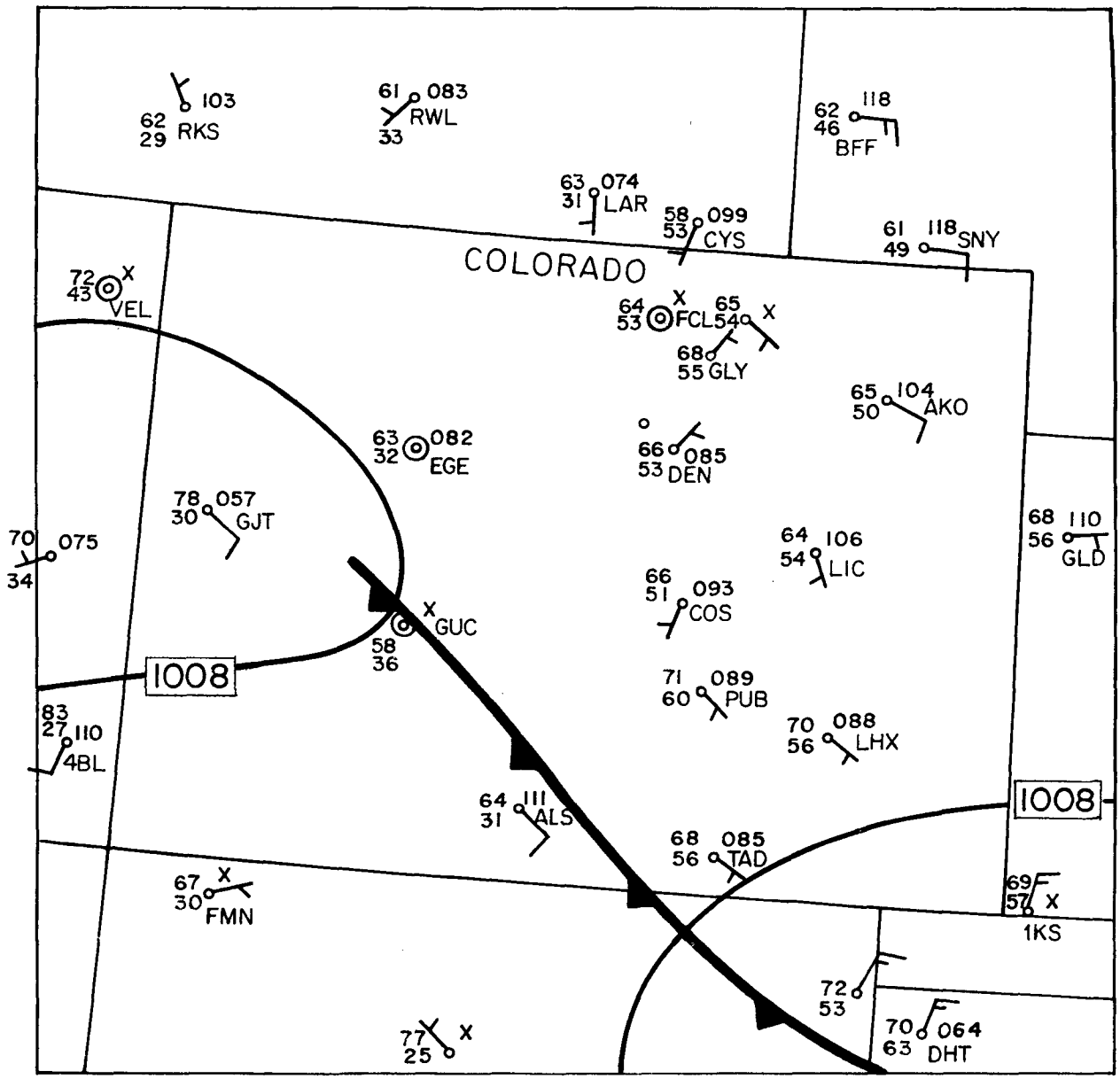

FIG. 5. Standard NWS surface observations from 0800 LST 6 June 1990 for Colorado and its vicinity with data from three PROFS mesonet sites (solid dots) added. The analysis (including frontal position) is taken from the NMC 0800 LST analysis chart. Station models and all symbols are conventional (Fig. 1d).

ture along the Front Range, with very dry air over the mountains inhibiting convective development there. Last, animated satellite imagery reveals that small convective elements that formed over, and just east of, the mountains evaporated quickly. This included most of the congestus that formed along the DCVZ. The cumuli generated along the DCVZ that did survive did not grow substantially until they had traveled 40–65 km (25–40 miles) eastward into what was evidently deeper moisture. Thus, indications were that the shallow moist layer had not deepened along the northern Front Range, even as late as midday.

As already noted, by 1301 LST a cluster of DCVZ congestus had finally developed into a second group of small thunderstorms situated just northwest of LIC (crosshair in Fig. 10). By this time, the western boundary of the cool, moist, low-level air that had been generated by overnight convection stretched from near CYS to roughly 90 km (55 miles) east of LIC. Cloud-tracking algorithms, applied to the western edge of the stratocumulus billows in sequential satellite imagery,

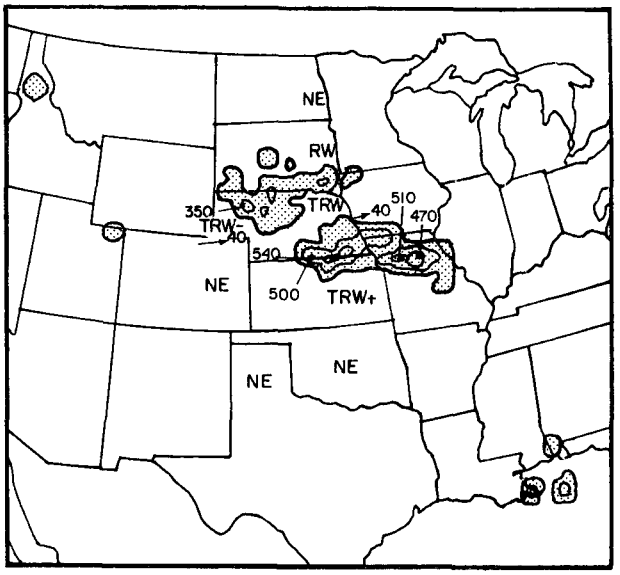

FIG. 6. NMC manually digitized radar chart from 0335 LST 6 June 1990. Shaded areas are regions where NWS surveillance radars detected precipitation echoes. Contours represent regions where reflectivity levels were 0–30, 31–40, and 41–49 dBZ, respectively. Three-digit numbers represent maximum echo tops in hundreds of feet.

showed that this boundary was moving toward the west at 5–8 m s^{-1} (10–15 kt).

b. 1300—1430 LST

Within an hour of its initial development, the convective activity northwest of LIC evolved into a large thunderstorm (storm labeled "1" in Fig. 12). Also, the DCVZ-generated activity (labeled "2" in Fig. 12) was located just to its northwest. By 1400 LST, Mile-High Doppler radar (MHD) detected reflectivities approaching 60 dBZ in both these cells (Fig. 13). Both storms were moving toward the east-northeast during this time period. Furthermore, by 1430 LST a third thunderstorm (labeled "3" in Fig. 12) was developing as a cluster of congestus south of Denver near the junction of the Front Range and the apex of the Palmer Lake Divide. This activity was in a location more typical for first convection along the Palmer Lake Divide, indicating that a deeper layer of low-level moisture may have been moving westward.

The 1400 LST MAPS analysis of 1500-m pressures (Fig. 14) reveals an increasing pressure gradient (compare Fig. 11) across the eastern plains of Colorado. Indeed, upslope surface winds had been strengthening since morning, which could account for the apparent

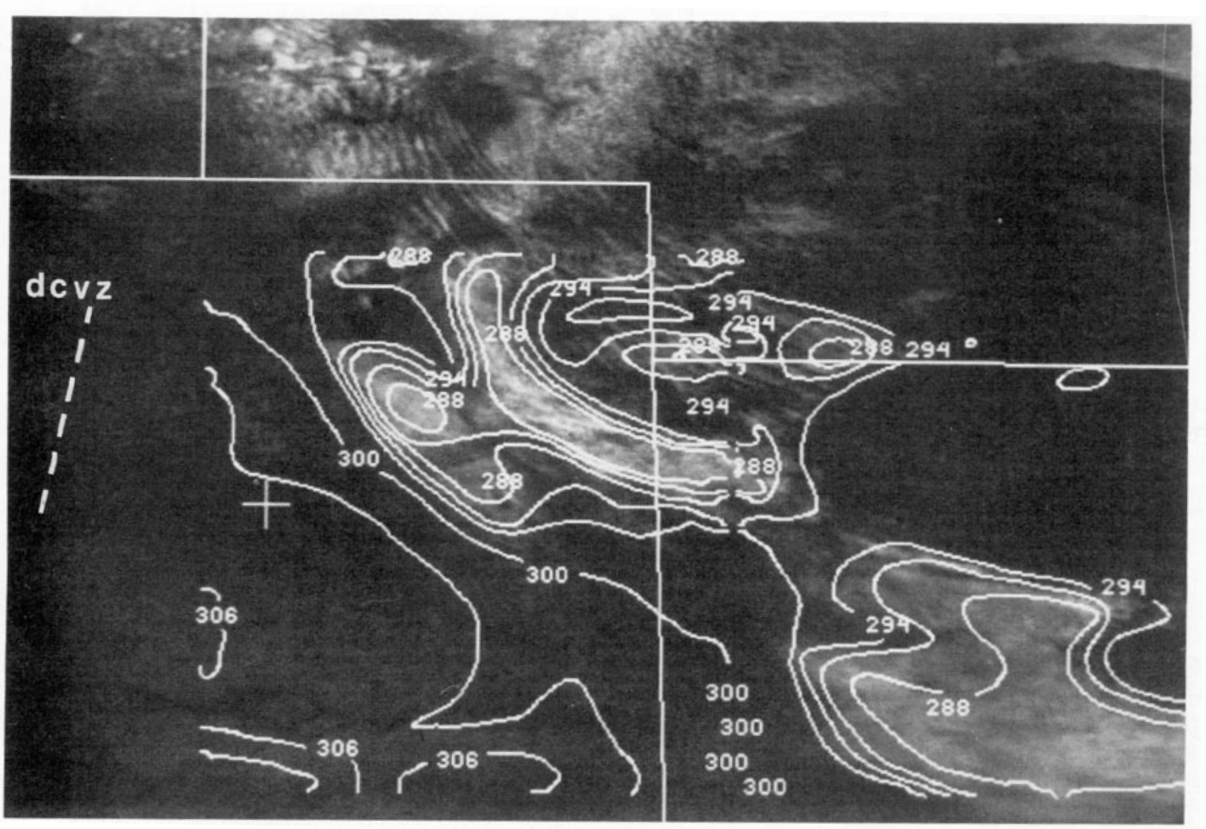

FIG. 7. *GOES-7*, 1-km visible image from 1001 LST 6 June 1990. The dashed line shows the approximate, normal location of the Denver Convergence and Vorticity Zone. *Goes-7*, 11-μm infrared temperature values in degrees kelvin have been superimposed. The crosshair is centered at Limon.

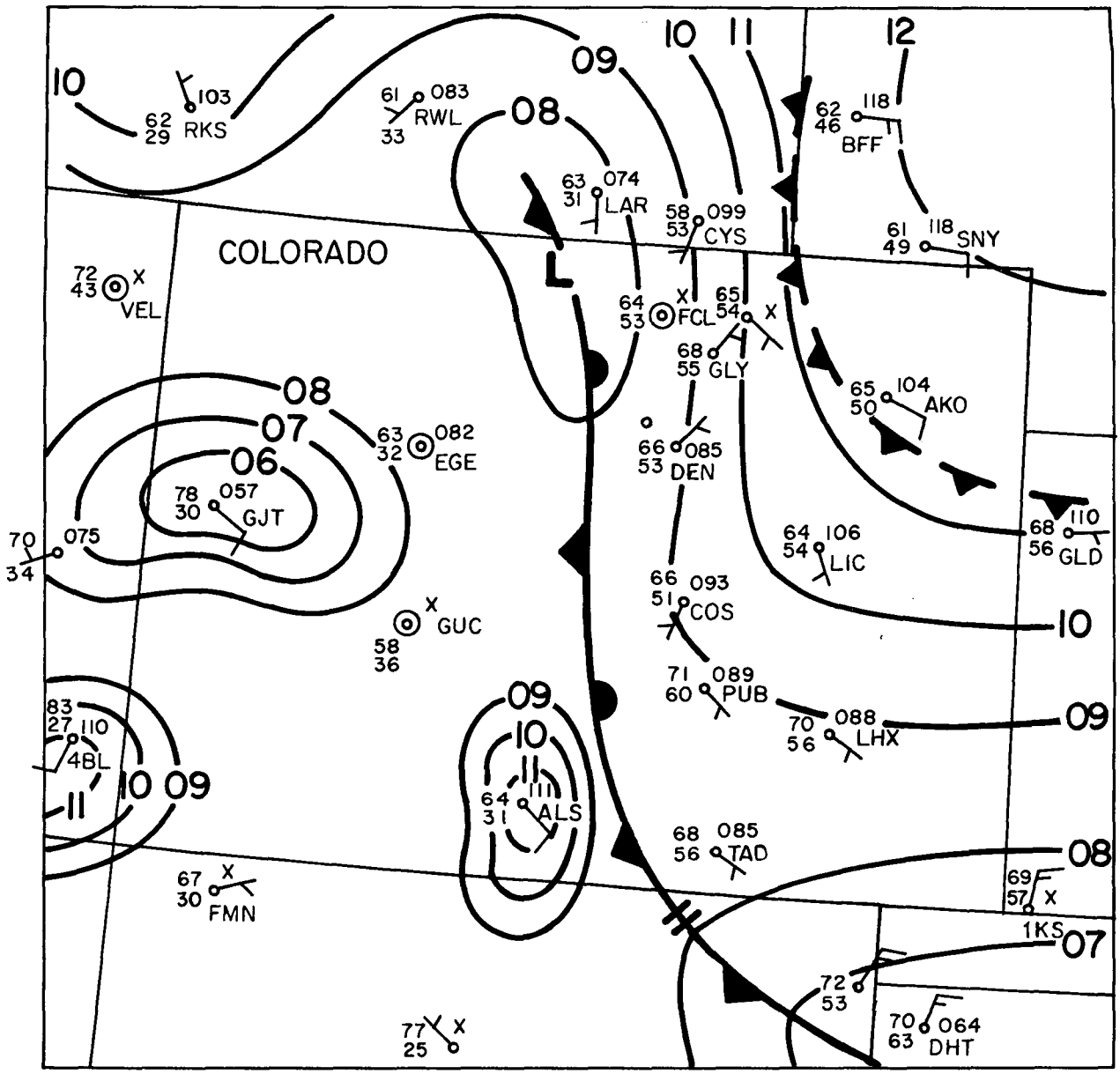

FIG. 8. Same as Fig. 5 except that a reanalysis has been carried out at 1-mb pressure increments. Subjective interpretation has also been incorporated based upon supplemental radar and satellite information and with a specialized knowledge of how weather features interact with local terrain. The mesoscale, frontogenetic symbol in northeastern Colorado represents the mesoscale outflow boundary as described in text.

westward progression of the low-level moisture noted above. Notice that the dewpoint analysis, using standard surface observations alone, finds a relatively uniform moist air mass on the plains. However, when data from mesonet stations are added and a subjective analysis is carried out, much more detail in this crucial field may be seen (Fig. 15). For example, a dry slot over the Palmer Lake Divide northwest of LIC is quite evident.

During this period, the stable mesoscale air mass associated with the earlier Kansas–Nebraska convection continued to move west at 5–8 m s^{-1} (10–15 kt). An objective, linear extrapolation algorithm run for the period 1230–1330 LST suggested that the leading edge of this air mass would intersect both storms 1 and 2 within the hour and would reach the LIC vicinity around 1645 LST.

Thus, by midafternoon, satellite imagery and surface observations were clearly indicating a convectively favorable region along and near a narrow corridor of low-level moisture situated between dry air along the Front Range and a stable air mass associated with the

mesoscale outflow boundary farther to the east. There were already active storms in that corridor. However, like most severe weather situations, there were complicating factors. First, there was continuing indication of a DCVZ in the mesonet observations (Fig. 15)—a bothersome feature that could tend to pull attention away from the situation developing near LIC. Also, notice the increasing dewpoints at several foothill stations (Figs. 9 and 15). This tendency points to a moistening boundary layer closer to the Front Range, complicating the forecast situation by introducing concerns for activity along and near the foothills. However, animated satellite imagery showed a continuing proclivity for convection to dissipate along the northern Front Range, allowing the short-range forecaster to put thoughts of the Denver metropolitan region on the back burner for a little while.

4. Mid-to-late afternoon

a. 1430—1530 LST

Storm 1 began to dissipate between 1400 and 1430 LST as it encountered the stable mesoscale air mass associated with the earlier Kansas–Nebraska activity. A close review of reflectivity data from the LIC WSR-57 surveillance radar (as viewed on 16-mm movie film) shows that as storm 1 moved east it left behind a faint thin line marking a line of shallow cloudiness along the edge of its own outflow (line 1, Fig. 16). As the storm began to dissipate, this thin line became much more distinct, due, most likely, to a sudden reinforcement of the cold outflow air.

Meanwhile, storm 2 had been traveling along behind storm 1, to its northwest. MHD radial velocity data (not shown) depicted a weak, 10–15-km (6–8 nmi) wide circulation at lower scan elevations. Limon radar summaries reported that storm motion was from 260° at 15 m s^{-1} (30 kt). At about 1450 LST the updraft region of storm 2 ran into the edge of the outflow left behind by storm 1 (thin line 1, Fig. 16). At this point, storm 2 turned right and began to propagate to the southeast. By 1512 LST, the reflectivity of storm 2 (Fig. 17) had reached 65 dBZ and velocity data (not shown) indicated that the low-level circulation had intensified.

During this period, storm 3 continued moving eastward at about 8 m s^{-1} (15 kt). By 1530 LST it was situated 112 km (70 nmi) west of LIC, and its core exceeded 50 dBZ.

Most of the activity near Limon on 6 June was observed by various on-site meteorologists (see acknowledgments). Their information yields additional insight into the unfolding events. In the case of storm 2, these observers reported that two tornadoes formed at 1515 LST near the small town of Deer Trail. The vortices were characterized as being narrow, weak, and short lived. The maximum duration on the ground for either tornado was "a couple of minutes." Furthermore, these observers reported that shortly after the second tornado

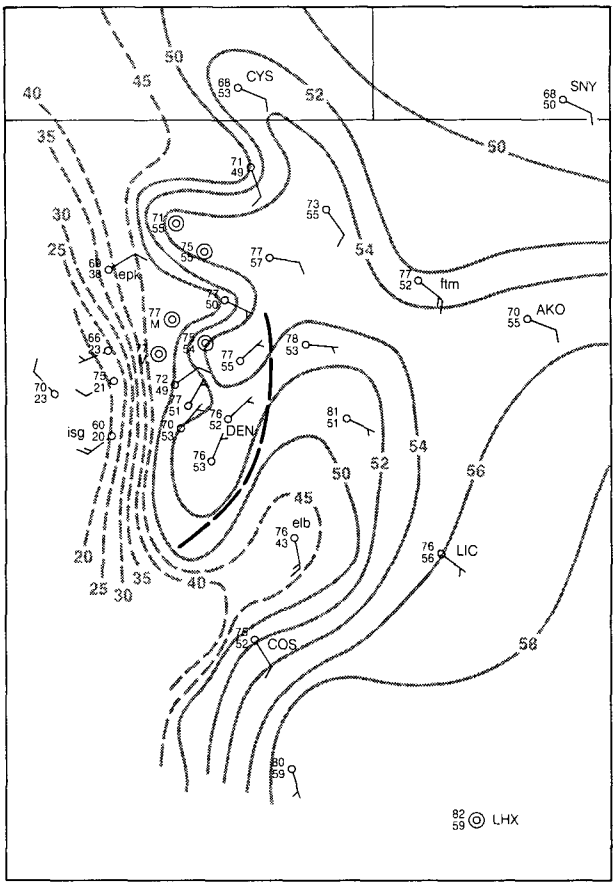

FIG. 9. MAPS analysis of surface dewpoints in increments of 2°F for dewpoints greater than 50°F (5°F increments otherwise) for 1100 LST 6 June 1990 over northeastern Colorado. Station models and all symbols are conventional. Wind barbs are as described in Fig. 1. The thicker dashed line shows the convergence boundary associated with the DCVZ.

dissipated, the visual appearance of storm 2 changed from that of a fairly standard, severe weather–producing cumulonimbus (e.g., Doswell 1985) to that of a bell-shaped storm of the type most often associated with low precipitation (LP) rates—that is, an LP supercell storm (Bluestein and Woodall 1990). However, it is important to note that storm 2 did not display other LP characteristics. The storm had a large reflectivity core that contained moderate-to-heavy precipitation. Also, it produced a fairly substantial downdraft at the surface.

It is interesting to speculate here on the nature of storm 2 and on some possible reasons for its associated tornadic activity. Such a discussion at this point might yield useful insights into the activity on 6 June from a forecast point of view.

Though a few aspects of storm 2 seem similar to those of classic, right-moving supercells (e.g., Browning 1964), there were many other aspects to suggest this was not the classic case. Most importantly, the deviate

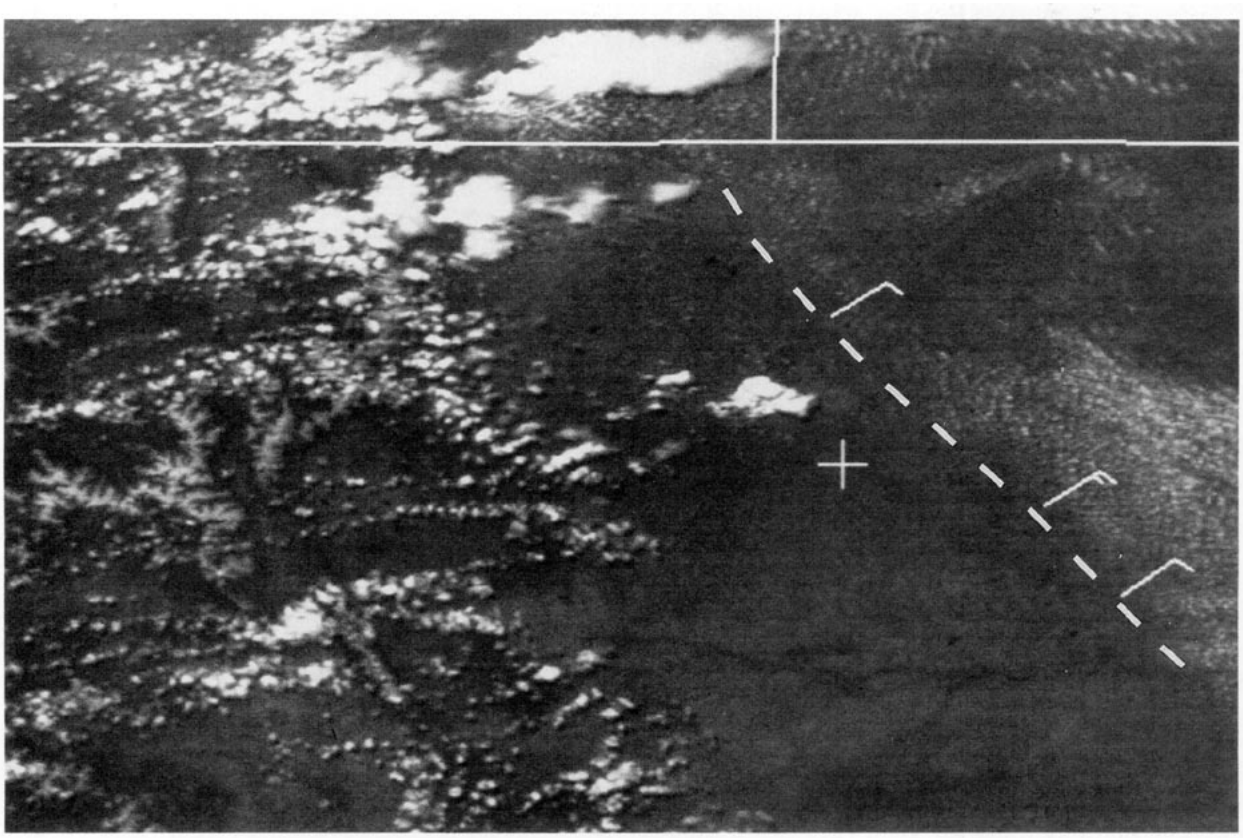

FIG. 10. *GOES-7*, 1-km visible image taken at 1301 LST 6 June 1990. The dashed line represents the leading edge of the mesoscale outflow region, and wind barbs indicate the westward translation vector. The crosshair is centered at Limon.

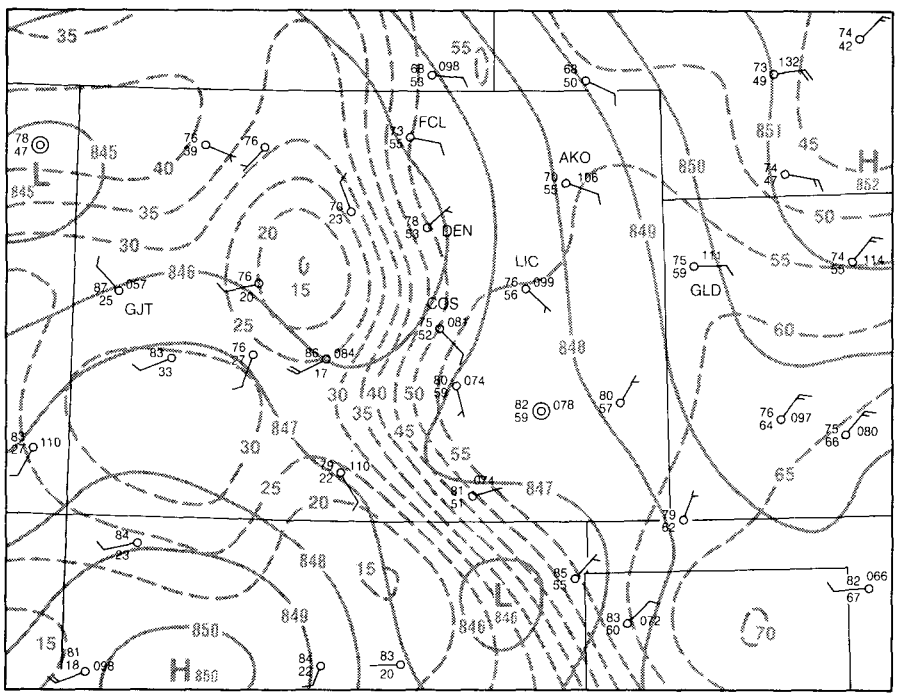

FIG. 11. Same as Fig. 3 except the map is for 1100 LST 6 June 1990.

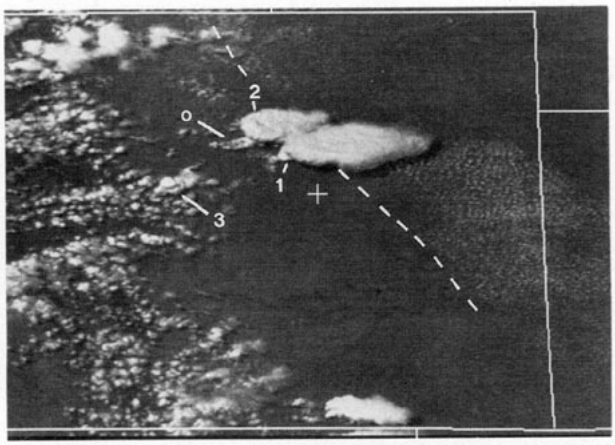

FIG. 12. *GOES-7*, 1-km visible image taken at 1401 LST 6 June 1990. The dashed line represents the leading edge of the mesoscale outflow region. Storms 1, 2, and 3 are as labeled. The region labeled "o" is the outflow from storm 2. The crosshair is centered at Limon.

motion seems to have been associated with the outflow from another storm and not storm-induced dynamics. However, the possibility of a supercell hybrid (one combining both factors) cannot be ruled out, since (as noted in section 2) the storm-relative helicity within the large-scale environment at this time and location was becoming more favorable for the development of thunderstorm mesocyclones. Additionally, the low-level winds along and just northeast of the outflow boundary would likely be from a more easterly direction as compared to the winds outside the outflow that tended to be from the southeast. Since the modified winds are backed relative to the larger-scale environmental flow, a more pronounced veering with height would occur along the outflow boundary bringing enhanced helicity on the local scale. Note also that once storm 2 turned to the right the *storm-relative* helicity would increase even further.

Outflow interaction may also have contributed to tornado formation. One way for this to occur would be for the horizontal vorticity associated with the edge of the cold outflow from storm 1 to be tilted into the vertical by the storm 2 updraft [similar to the mechanism described by Rotunno and Klemp (1985)]. A second possibility is that preexisting vertical vortices along the gust front could have been drawn into the storm 2 updraft in the manner of Wilson et al. (1992). Neither of these mechanisms would require a supercell environment in order to occur.

Another reasonable explanation for tornado occurrence, and one that fits the known facts, is the possible concentration of existing vorticity through the stretching of the middle levels of the storm 2 updraft. In this case, the sequence of events would unfold as follows. The mildly rotating storm, after encountering strong outflow from storm 1, begins to propagate southeastward along the outflow. However, because the mean environmental flow (3–10 km depth) was from the west-southwest, the storm would have a continuing tendency to move eastward across the lower CAPE air associated with the outflow from storm 1. As the storm ingested this lower-energy air, the vertical velocity in the lower part of the storm would necessarily decrease. However, for a short period, the velocities aloft would still be large (due to conservation of momentum), so the updraft would elongate and, by continuity, narrow. Then, by conservation of angular momentum (or, alternatively, conservation of potential vorticity), a brief "spinup" of the circulation could occur.

Both the "ingesting of pre-existing vertical vortices" and the "choking-off of storm 2's updraft" explanations are consistent with the weak, short-lived nature of the observed tornadoes. However, the second scenario might also help explain the LP appearance of the storm during this phase. The conical shape (i.e., a wide updraft base, narrowing to a thin, laminar cloud at midlevels) may have been an indication of the stretching of the rotating updraft at midlevels. In fact, though speculation may be instructive and interesting, it is not really possible to determine exactly what mechanisms were at work during this brief period of storm 2's life. This slight digression was meant simply to provide food for thought regarding the problem of storm-outflow interactions.

The tornadic phase of storm 2 lasted less than an hour. Thirty minutes later, as the cell reached the cool, mesoscale air mass, it began to weaken and die.

b. 1530—1700 LST

As storm 2 moved southeastward into the mesoscale air mass, its reflectivity core weakened and a large region of newly formed, rain-cooled air appeared to its west in visible satellite imagery. This feature manifested itself as a curved line of cumulus cloud surrounding a clear region ("o" in Fig. 18). The line of cumulus also corresponded to a faintly visible thin line on MHD radar (Fig. 17) and to the feature marked "thin line 2" in Fig. 16. The feature was trackable on animated satellite imagery from 1500 to 1546 LST but was lost beneath the anvil of storm 3 after that time. Subsequently, it could be followed in the MHD radar reflectivity data (Figs. 19 a–d) as a thin line at lower-elevation scans. Between 1630 and 1700 LST, this thin line appeared to sweep across storm 3 from the north. Figure 19d clearly shows a portion of this line to the east of storm 3.

Also during this time period, animated satellite imagery indicated that the mesoscale air mass that had been moving westward all day slowed down and finally stopped just to the east of Limon. The significance of this will be discussed later.

c. 1700—1930 LST

Storm 2 weakened substantially just after 1700 LST, and storm 3 became the focus of attention. The line

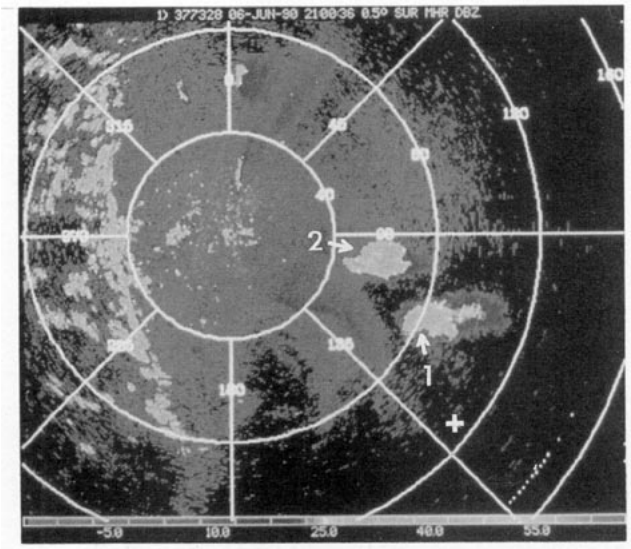

FIG. 13. MHD, 0.5° surveillance scan, reflectivity data from 1400 LST on 6 June 1990. Range rings are at 40-km increments; the reflectivity is scaled in dBZ. MHD radar is located just northeast of DEN (small dot in Fig. 2). Storms corresponding to storms 1 and 2 in Fig. 12 are indicated, and the crosshair is centered at LIC. Note: most of the echo on the west side of the scope is ground clutter from the Front Range of the Rocky Mountains.

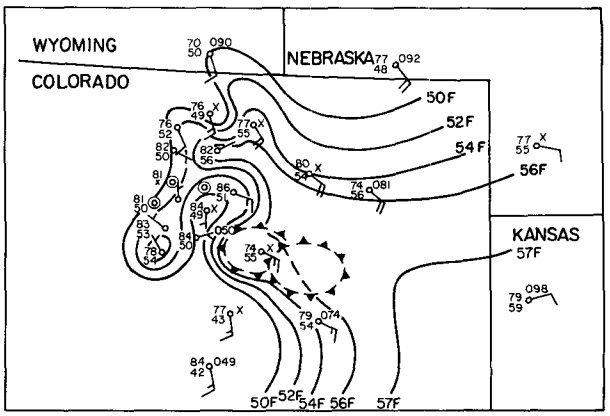

FIG. 15. Analysis of surface dewpoints (in 2°F increments) from 1400 LST 6 June 1990. Small, ring-shaped cold areas near the center of the analysis depict the thunderstorm outflow regions as shown on GOES visible imagery (e.g., Fig. 12).

of cumulus along the advancing edge of the outflow from storm 2 became very well defined on visible satellite imagery and the thin line of reflectivity on MHD radar brightened as it began pushing rapidly southward. Small, intense cores (reflectivities 30–45 dBZ; diameters of 3–5 km) developed within and just to the east of storm 3 as the outflow swept into the region. This was the most intense outflow signature on radar throughout the afternoon. Also, observations by onsite meteorologists just south of storm 3 reported a line of developing towering cumulus that stretched northeast from the updraft region (i.e., the southwestern flank) at this time. Farther to the northeast, convection developed enough to produce small rain showers. This

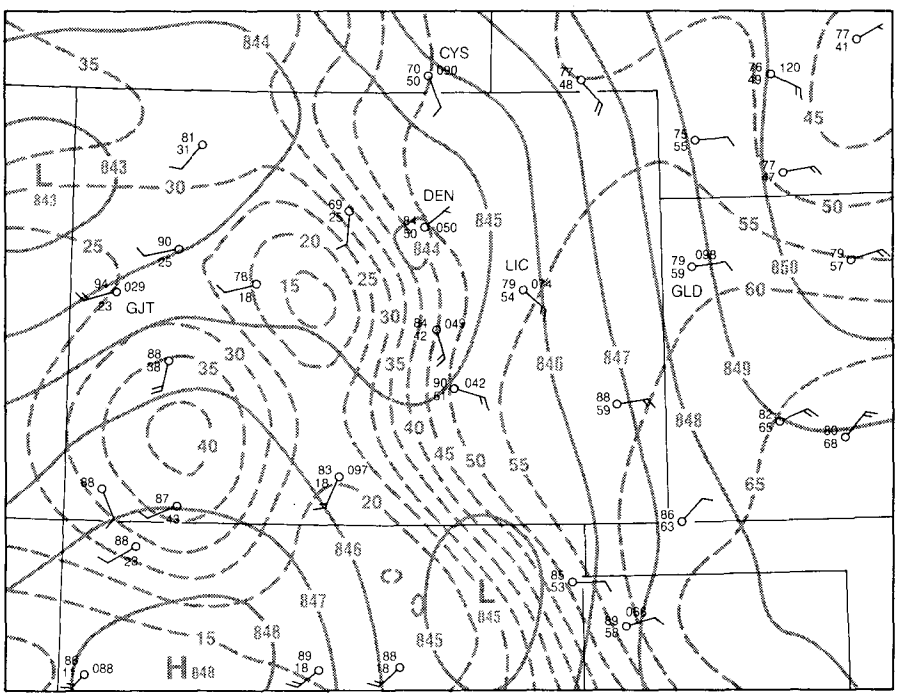

FIG. 14. Same as Fig. 3 except the map is for 1400 LST 6 June 1990.

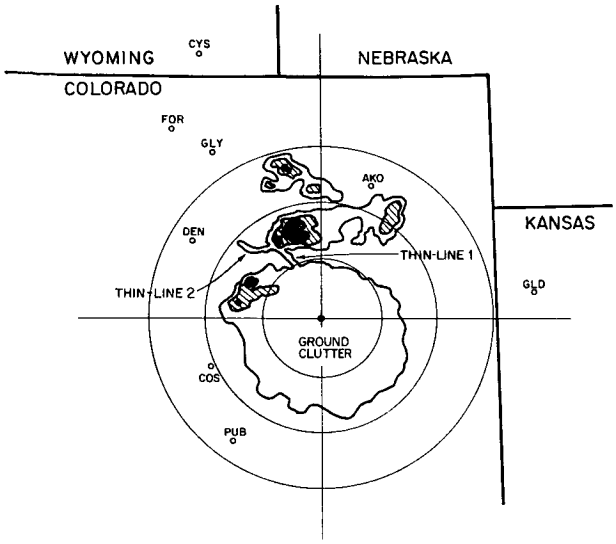

FIG. 16. The drafted version of a tracing taken from the 16-mm film of the LIC radar scope at approximately 1450 LST. Range rings are at 46.3-km (25 nmi) intervals. Echo intensities represented are 0–29 dBZ (unshaded), 30–40 dBZ (lined), 41–45 dBZ (stippled) and greater than dBZ solid. (Note: the 16-mm film quality was too poor to reproduce directly.)

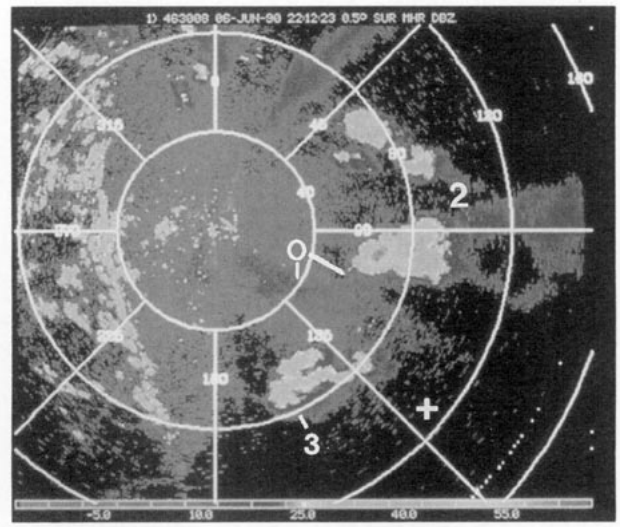

FIG. 17. MHD 0.5° surveillance scan, reflectivity data from 1512 LST on 6 June 1990. Range rings and reflectivity scaling as in Fig. 13. The thin line associated with the leading edge of the outflow is indicated by the letter "o". Storms 2 and 3 are labeled. The crosshair is at LIC.

observation is consistent with the line of small echoes seen on radar reflectivity data.

Following the apparent interaction (between about 1630 and 1645 LST) with storm 2's outflow, storm 3 intensified dramatically. Its areal extent increased by about 40% on the MHD radar, its reflectivity increased by about 15 dBZ, and it developed a hooklike appendage on the southwest edge of its low-level echo. Hook echoes are frequently associated with thunderstorms having mesocyclones (e.g., Forbes 1981). On-site observers reported the development of a rotating wall cloud within a half hour of this time, and the MHD velocity scans showed an organized circulation developing at low levels.

Due to the intervening echo, it is impossible to establish with certainty a definitive connection between the intrusive outflow from storm 2 and the intensification of storm 3, but the coincidence seems fairly convincing. Many such interactive intensifications have been documented over the years (e.g., Purdom 1976). Also, modeling studies have suggested that horizontal vorticity associated with a supercell's front flank downdraft (FFD) can be drawn into its own updraft to produce strong, low-level rotations about the vertical (Rotunno and Klemp 1985). In this case, it is likely that the outflow from storm 2 reinforced storm 3's FFD, making this effect even more significant.

At about 1810 LST, on-site meteorologists reported a large tornado touching down several kilometers southwest of LIC (Fig. 20). The tornado remained on the ground for about 15–20 min. Its strength was reported as F3 (NOAA 1990), although it occurred over sparsely populated areas making damage assessment difficult.

Meteorologists observing storm 3 reported that this tornado dissipated as rain wrapped cyclonically around it. That is, the mesocyclonic circulation associated with the storm's updraft appeared to occlude. However, the line of developing towers to the east of the rain area remained a steady feature relative to the storm, joining the "rain-free" updraft on its eastern edge. Thus, the potential source of horizontal vorticity remained in place. As the storm continued toward Limon, 4.5–6.3-cm (1.75–2.5 in.) diameter hail fell at the National Weather Service (NWS) radar site several kilometers south of the town. Shortly before 1900 LST a second

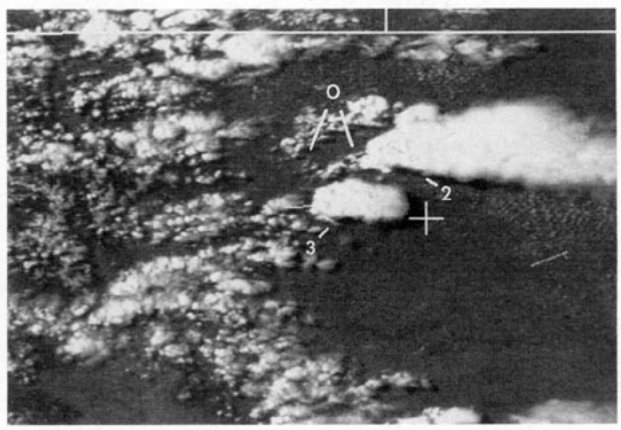

FIG. 18. *GOES-7*, 1-km visible image from 1501 LST on 6 June 1990. Outflow to the west of the northernmost storm is indicated by the letter "o." Storms 2 and 3 are as labeled. The crosshair is at LIC.

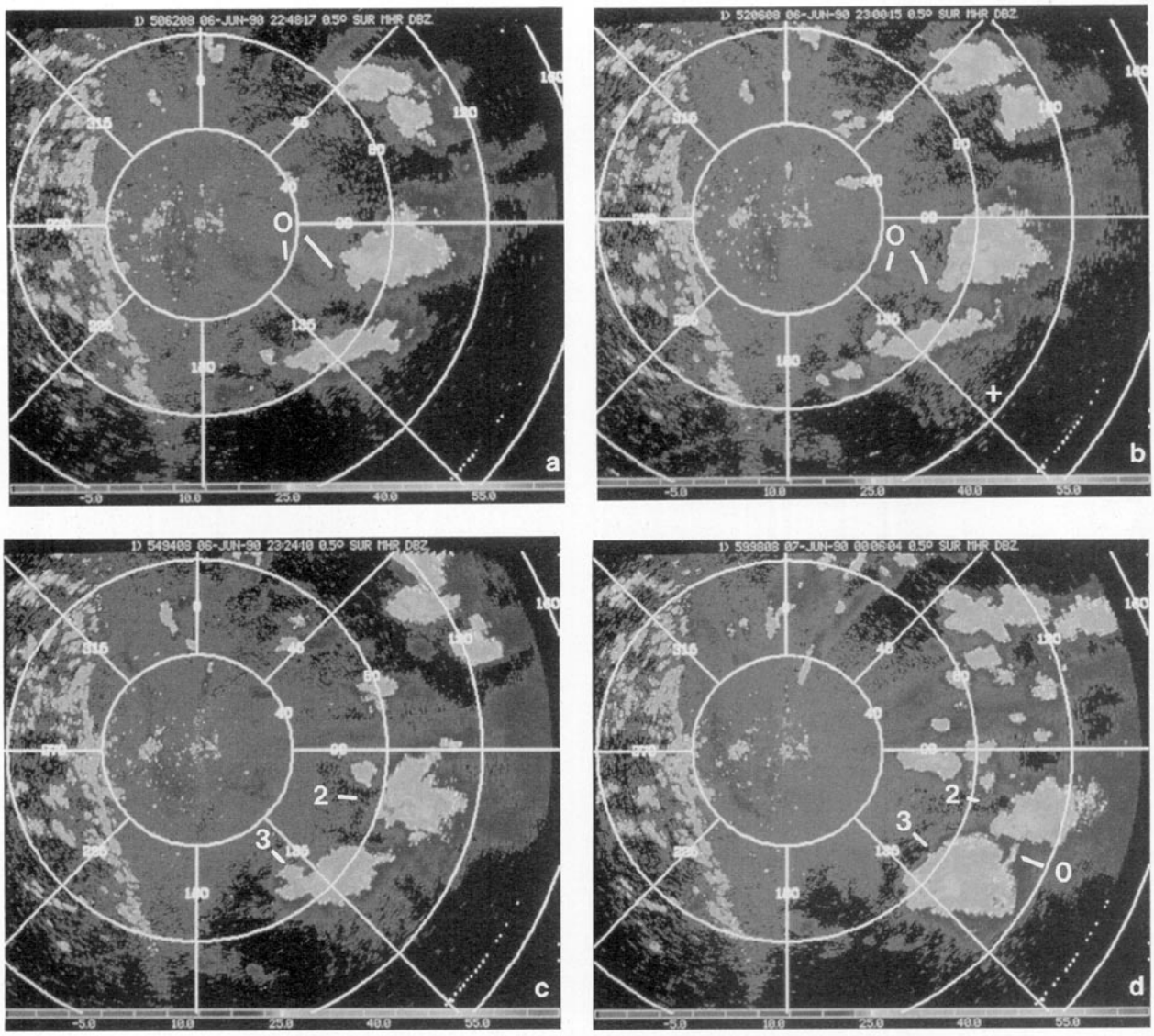

FIG. 19. MHD 0.5° surveillance scan, reflectivity data from various times on 6 June 1990. Range rings and reflectivity scaling as in Fig. 13. Shown are (a) 1548 LST—"o" indicates the leading edge of the outflow from storm 2, (b) 1600 LST data with crosshair indicating location of LIC, (c) 1624 LST—storm numbers 2 and 3 as indicated, and (d) 1706 LST—"o" indicates the leading edge of outflow from storm 2 as it sweeps through storm 3.

F3 tornado touched down, moving into Limon at 1908 LST. Damage approaching F4 intensity was produced along the town's main street. At this time the MHD radar measured a strong, cyclonic shear (roughly 30 ms^{-1} over a distance of 2 km) in the lowest elevation scans.

Figure 21 is an enlargement of the 0.5° reflectivity data just prior to the time of development of the second tornado. It clearly shows the hook-echo pattern often associated with tornadic storms. Note also that the visible satellite image (Fig. 22) reveals many of the characteristics associated with severe thunderstorms (such as the overshooting tops and above-anvil cirrus plumes). Infrared imagery reveals corresponding cold tops and warm wakes throughout the afternoon. At the time of the tornado, no easily recognizable cold top was in evidence, although a large, poorly defined warm wake had developed. The warm wake was surrounded by a cold, horseshoe-shaped cold area (Fig. 23). [For a complete discussion of severe thunderstorm cloud-top characteristics observed in satellite imagery, see Heymsfeld and Blackmer (1988).]

Shortly after the destructive tornado moved out of LIC, it dissipated. On-site meteorologists reported observing what they referred to as "low-level, cold looking stratocumulus" moving into the storm from the east. Subsequent interviews, together with visible satellite imagery, confirm that storm 3 had intercepted the me-

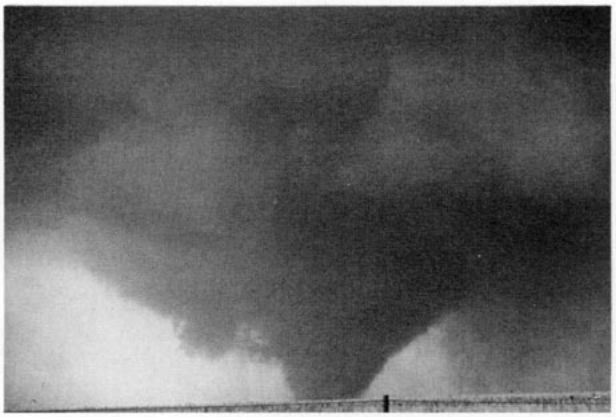

FIG. 20. Tornado on the ground near Matheson, Colorado (12 miles southwest of LIC) at approximately 1810 LST on 6 June 1990. National Center for Atmospheric Research photo courtesy of E. W. McCaul, Jr.

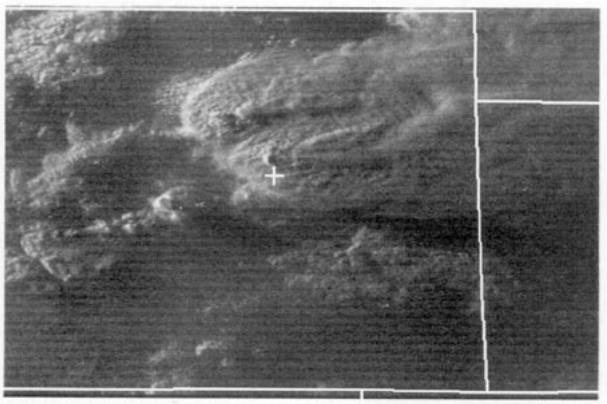

FIG. 22. *GOES-7*, 1-km visible image from 1846 LST on 6 June 1990. The crosshair is at LIC.

soscale air mass that had been created the night before. This air mass was still capped by a relatively thick field of billow clouds and was apparently still too stable to support strong convection. Thus, it is relatively certain that had the stable air continued westward just a few more kilometers, LIC might have been spared its later tragedy.

Thunderstorms continued to occur west of LIC for several hours after dark. There were reports of large hail just east of both Denver and Colorado Springs. There were also four other tornadoes reported, three F0s and one F2, all east of Colorado Springs. However, very few data are available for the nighttime events, so a discussion of this activity will not be presented.

5. Concluding remarks

A complex series of events combined to produce severe weather over the plains of Colorado on the afternoon and evening of 6 June 1990. In addition to a synoptic pattern that was favorable for High Plains severe thunderstorms (Doswell 1980), there was an unusually unstable air mass over eastern portions of the state. A vertical wind shear profile favorable for severe thunderstorms developed during the day.

Strong thunderstorms occurred throughout much of northeast Colorado and southeast Wyoming, but several mesoscale mechanisms served to concentrate the most severe activity into a small portion of the larger, synoptically favored region. The sequence of events unfolded as follows.

1) Stable low-level outflow air from overnight thunderstorms in Kansas and Nebraska moved into northeastern Colorado, covering large portions of the region with a "capped," thermodynamically stable air mass.

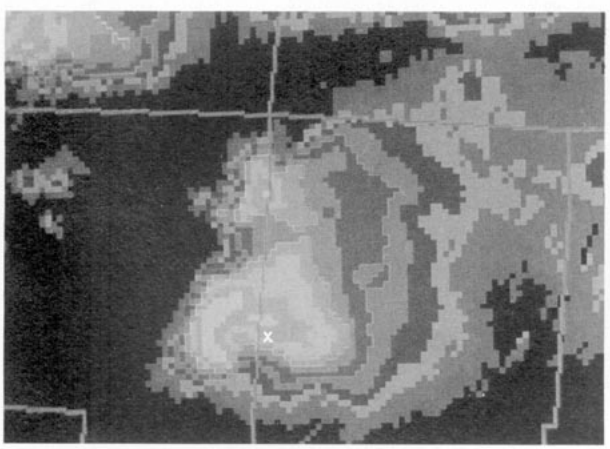

FIG. 21. Close-up of MHD 0.5° surveillance scan, radar reflectivity data from 1836 LST (just before the Limon tornado) on 6 June 1990 showing the hook-echo configuration. Limon is located at "X."

FIG. 23. *GOES-7*, 4-km infrared image from 1846 LST on 6 June 1990. A poorly defined cold edge around the perimeter of the Limon storm is indicated by the letter "U" and arrows. The region downwind from this edge is 12°C warmer and is associated with the above-anvil cirrus seen in Fig. 17.

2) The air mass over the Rocky Mountains, as well as a narrow slot along the Front Range, was apparently too dry to support deep convection throughout most of the day.

3) Thunderstorms that formed and/or moved east of the Front Range dry slot intensified as they crossed into the convectively more favorable region of low-level moisture just east of Denver. They continued to move eastward and intensify until they encountered the stable, mesoscale air mass formed by the Kansas and Nebraska activity the night before. At that point, they weakened appreciably. However, this weakening caused further interactions to occur. The first storm to encounter this air mass and weaken (storm 1) produced a strong outflow that then interacted with another storm to form two small tornadoes.

4) Outflow that formed when the second storm weakened is thought to have reinforced the forward flank downdraft of a third large cell resulting in the formation of two F3 tornadoes, one of which produced major damage in Limon.

The presence of mesoscale thunderstorm outflow air masses lasting far beyond the convective event is not unique. Such air masses can propagate considerable distances from their parent storm complexes. For example, Weaver and Toth (1990) found that outflow from overnight convection in Kansas and Nebraska played an important role in the extremely damaging hailstorm outbreak that occurred along the Front Range on 2 August 1986. In that case, the mesoscale air mass acted in a more positive manner, providing a slightly capped but extremely unstable source of energy for storms that formed in the Front Range corridor. It is interesting that even though the mesoscale air mass in the current study acted to weaken individual convective elements its ultimate effect was to enhance the overall severity of the Limon event.

The Doswell (1980) criteria for determining the likelihood of severe thunderstorms occur frequently in north-central Colorado, as does the DCVZ. Yet occurrences of very large hail and large tornadoes are relatively rare and isolated. Even when they do occur, the affected area is quite small as compared to the total area threatened. Thus, it makes sense to look for additional forcing mechanisms and/or limiting factors for severe convection when such activity is anticipated. However, NMC surface analyses are not intended to provide details on the mesoscale (Uccellini et al. 1992). The forecaster is faced with the problem of having to analyze extremely complex mesoscale situations in what often turns out to be minutes. Detailed and careful subjective reanalysis of surface observational data is frequently not practical. At such times, remote sensor data, such as satellite imagery or radar information, can often provide a quick, analog overview of a rapidly evolving weather event. The sampling of other data presented in the current study shows how important this can be (e.g., why the DCVZ-generated convection did not intensify until it had traveled several tens of kilometers to the east).

Last, if additional mesoscale features can be identified on a day when overall synoptic conditions are favorable for severe development, forecasters should be alert to the possibility of especially significant storms. Attention should be given to apparent airmass differences and to places where existing convection might encounter boundaries separating different air masses.

Acknowledgments. A portion of the research described in this paper was performed under NOAA Grant NA85RAH050345. The authors would like to thank Cindy Mueller and Dan Megganhart (both of NCAR) for providing Mile-High Doppler radar slides for this case. Thanks are also due D. Blanchard (National Severe Storms Laboratory, Boulder office) and M. Weisman (NCAR) for their patience through several discussions concerning their personal observations of events on this day. Humberto Rodriguez (Colorado State University) furnished helpful analyses and discussions. The NCAR photo of the Matheson, Colorado, tornado was provided by E. W. McCaul, Jr. Finally, we would like to express our thanks to the reviewers of this work for the time they spent to make this paper a much more interesting study.

REFERENCES

Benjamin, S. G., and P. A. Miller, 1990: An alternative sea level pressure reduction and a statistical comparison of geostrophic wind estimates with observed winds. *Mon. Wea. Rev.*, **118,** 2099–2116.

Bluestein, H. B., and G. R. Woodall, 1990: Doppler-radar analysis of a low-precipitation severe storm. *Mon. Wea. Rev.*, **118,** 1640–1664.

Browning, K. A., 1964: Precipitation and airflow trajectories within severe local storms which travel to the right of the winds. *J. Atmos. Sci.*, **21,** 634–639.

Davies-Jones, R., D. Burgess, and M. Foster, 1990: Test of helicity as a tornado forecast parameter. *Proc. 16th Conf. Severe Local Storms,* Kananaskis Park, Alberta, Canada, Amer. Meteor. Soc., 588–592.

Doswell, C. A., III, 1980: Synoptic-scale environments associated with High Plains severe thunderstorms. *Bull. Amer. Meteor. Soc.,* **61,** 1388–1400.

——, 1985: The operational meteorology of convective weather. Volume II: Storm scale analysis. NOAA Tech. Memo. ERL ESG-15, 240 pp.

Forbes, G. S., 1981: On the reliability of hook echoes as tornado indicators. *Mon. Wea. Rev.*, **109,** 1457–1466.

Fujita, T. T., 1971: Proposed characterization of tornadoes and hurricanes by area and intensity. Satellite and Mesometeorology Research Project (SMRP) Research Paper, No. 91, The University of Chicago, 42 pp.

Heymsfeld, G. M., and R. H. Blackmer, Jr., 1988: Satellite-observed characteristics of midwest severe thunderstorm anvils. *Mon. Wea. Rev.*, **116,** 2200–2224.

Klitch, M. A., J. F. Weaver, F. P. Kelly, and T. VonderHaar, 1985: Convective cloud climatologies constructed from satellite imagery. *Mon. Wea. Rev.*, **113,** 326–337.

Leftwich, P. W., Jr., 1990: On the use of helicity in operational assessment of severe storm potential. *Proc. 16th Conf. Severe Local*

Storms, Kananaskis Park, Alberta, Canada, Amer. Meteor. Soc., 306–310.

Miller, P. A., and S. G. Benjamin, 1992: A system for the hourly assimilation of surface observations in mountainous and flat terrain. *Mon. Wea. Rev.,* **120,** 2342–2359.

NOAA, 1990: Storm data and unusual weather phenomena with late reports and corrections. 32(6), NESDIS, National Climatic Data Center.

Purdom, J. F. W., 1976: Some uses of high-resolution GOES imagery in the mesoscale forecasting of convection and its behavior. *Mon. Wea. Rev.,* **104,** 1474–1483.

——, 1990: Convective scale weather analysis and forecasting. *Weather Satellites; Systems, Data, and Environmental Applications,* Amer. Meteor. Soc., 503 pp.

Rotunno, R., and J. Klemp, 1985: On the rotation and propagation of simulated supercell storms. *J. Atmos. Sci.,* **42,** 271–292.

Scofield, R. A., and J. F. W. Purdom, 1986: The use of satellite data for mesoscale analyses and forecasting applications. *Mesometeorology and Forecasting,* P. S. Ray, Ed., Amer. Meteor. Soc., 793 pp.

Szoke, E. J., and J. A. Augustine, 1990: A decade of tornado occurrence associated with a surface mesoscale flow feature—The Denver cyclone. *Proc. 16th Conf. Severe Local Storms,* Kananaskis Park, Alberta, Amer. Meteor. Soc., 554–559.

——, M. L. Weisman, J. M. Brown, F. Caracena, and T. W. Schlatter, 1984: A subsynoptic analysis of the Denver tornadoes of 3 June 1981. *Mon. Wea. Rev.,* **112,** 790–808.

Uccellini, L. W., S. F. Corfidi, N. W. Junker, P. J. Kocin, and D. A. Olson, 1992: Report on the surface analysis workshop held at the National Meteorological Center 25–28 March 1991. *Bull. Amer. Meteor. Soc.,* **73,** 459–472.

Weaver, J. F., and J. J. Toth, 1990: The use of satellite imagery and surface pressure-gradient analysis modified for sloping terrain to analyze the mesoscale events preceding the severe hailstorms of 2 August 1986. *Wea. Forecasting,* **5,** 279–298.

——, and N. J. Doesken, 1991: High Plains severe weather—Ten years after. *Wea. Forecasting,* **6,** 411–414.

Weisman, M. L., and J. B. Klemp, 1982: The dependence of numerically simulated convective storms on vertical wind shear and buoyancy. *Mon. Wea. Rev.,* **110,** 504–520.

Wilson, J. W., G. B. Foote, N. A. Crook, J. C. Fankhauser, C. G. Wade, J. D. Tuttle, and C. K. Mueller, 1992: The role of boundary layer convective zones and horizontal roles in the initiation of thunderstorms: A case study. *Mon. Wea. Rev.,* **120,** 1785–1815.